Chaotic neocortical dynamics.

Walter J Freeman
Department of Molecular & Cell Biology MC 3206
University of California at Berkeley CA 94720 USA
dfreeman@berkeley.edu http://sulcus.berkeley.edu

Ch. 22 in: Chaos, CNN, Memristors and Beyond. A Festschrift for Leon Chua. Adamatzky A, Chen G (eds.), Singapore: World Scientific, pp. 271-284.

Key words: basin-attractor dynamics; chaos; cortex; criticality; ECoG and EEG; meaning; perception; scale-free dynamics; semantics

Abstract

The first step of the sensory systems is to construct the meaning of the information they receive from the senses. They do this by generating random noise and then filtering the noise with adaptive filters. We simulate the operation with the solutions of matrices of ordinary differential equations that predict bifurcations between point and limit cycle attractors. The second step is integration of the outputs from the several sensory systems into a multisensory percept (gestalt), which in the third step is consolidated and stored as knowledge. Simulation of the second step requires use of landscapes of non-convergent *chaotic* attractors. This is not deterministic chaos, which is much too brittle owing to the infinite sensitivity to initial conditions. It is a hybrid form we call *stochastic chaos*, which is stabilized by additive noise modeled on noise sources in the sensory systems. Thus bifurcation and chaos theory provides tools for succinct empirical models of cortical dynamics performing the most basic cognitive operations: generalization, abstraction, and categorization in constructing knowledge. The descriptions are in a form that is suitable for more advanced modeling using analog VLSI, neuropercolation from random graph theory, non-equilibrium dissipative thermodynamics, and macroscopic many-body physics. This review concludes with a summary of the applications of stochastic chaos in pattern classification and some prescriptions for neurobiologists on what to look for in large-scale anatomical formations.

1. Introduction

1. A. Brain hierarchy of levels: microscopic, mesoscopic, macroscopic

This essay addresses two paradoxes stemming from the 1950s. On the one hand Claude Shannon (1948) in his preface to information theory famously wrote: “The fundamental problem of communication is that of reproducing at one point either exactly or approximately a message selected at another point. Frequently the messages have meaning; that is they refer to or are correlated according to some system with certain physical or conceptual entities. These semantic aspects of communication are irrelevant to the engineering problem (p. 384)”. Yet the main role of the sensory cortices is to construct the meaning of sensory information, so that semantics is at the core of neurodynamics. On the other hand the ceaseless, aperiodic, unpredictable activity we observe in cortex invites modeling with chaotic dynamics in order to exploit the capacity of chaotic dynamics to create enormous quantities of new information (Skarda and Freeman, 1987).

Yet deterministic chaotic systems are stationary, autonomous, and noise-free, whereas brains are drenched in endogenous and environmental noise; they are continually evolving through successive bifurcations; and they are necessarily engaged with the environment in the constant extraction of energy for oxidative metabolism and the dissipation of heat (Freeman and Vitiello, 2010). What are the uses of chaos theory, and how is it that it has become so useful?

Within the decade John von Neumann (1958) wrote: "Whatever the language of the brain is, it cannot fail to differ considerably what we consciously and explicitly consider as mathematics … . Brains lack the arithmetic and logical depth that characterize our computations. … We require exquisite numerical precision over many logical steps to achieve what brains accomplish in very few short steps" (pp. 80-81). Models of brain functions using the tools of computational neural networks and rule-driven symbol manipulation require many steps between input and output. Recent advances in nonlinear brain dynamics have emphasized the capabilities of brains for exceedingly rapid acquisition and filtering of relevant sensory information through all of the senses, followed by synthesis of the meanings of the information (Freeman, 2003a). Cortices condense the meanings into various forms of knowledge, and express them in natural languages. All these operations transcend the capabilities of contemporary machine intelligence. The aim of this essay is to review progress in using chaos theory to answer the questions in qualitative terms, how brains construct knowledge and meaning from sensory information.

Any explanation that strives to meet von Neumann's challenge must rely on connections among very large numbers of neurons in many areas of the brain. Topographic mapping by parallel arrays of axons provides sensory input and motor output with the fine structure that enables brains to discriminate precisely small changes in input as fine as single sensory receptors and to focus control of motor output even to single motor units. In contrast, the steps between microscopic sensory inputs and microscopic motor outputs require wide divergence and convergence of axonal and dendritic connections to encompass very many neurons. Then the first of the "few short steps" in brain function requires transition from sparse high-intensity of *microscopic* sensory information carried by very few neurons to low-intensity of perceptual information carried by *mesoscopic* assemblies of neurons (Freeman, 2003b). The requisite cognitive operations are generalization, abstraction and categorization.

This step taken by the sensory cortices is the construction of the meaning of the information. We postulate that the meaning of the information exists in the interrelations of the enormous number of neurons carrying each a fragment of information, which constitutes the knowledge brains create from information (Freeman, Gaál and Jornten, 2003). This knowledge must be stored and later mobilized in the serial processes for categorizing sensory information and then deciding on courses of action in response to the input. Mobilized knowledge has the form of bursts of oscillatory electroencephalographic (EEG) and electrocorticographic (ECoG) potentials carrying spatial patterns of amplitude modulation (AM) (Fig. 01, A), which emerge from chaotic oscillations of background activity (Freeman and Burke, 2003) through episodic bifurcations (state transitions) by which the cortex jumps from chaotic disorder into phase-locked limit cycle activity (Freeman and Rogers, 2003) and back again.

Fig. 01 near here

The penultimate step of taking action requires the reverse operations of speciation and concretization of the low density broadly distributed firing (Freeman, 2006, 2007), which occur by focusing of neural activity into high-intensity but sparse firing of neurons in strategic mesoscopic assemblies. The assemblies activate microscopic networks of neurons that integrate tactical motor commands with proprioceptive information, which is the sensory feedback from muscle receptor neurons firing rapidly and precisely as tasks are performed. The output of the relatively few motor neurons is by pulse trains that convey information at high specificity (Freeman, 2004a,b). We conceive von Neumann's "few short steps" as state transitions between these three levels: microscopic - based in microelectrode recordings; mesoscopic - based in intracranial arrays to record the electrocorticographic (ECoG) recordings; and macroscopic - based in scalp arrays to capture the electroencephalographic (EEG) and functional magnetic resonance imaging (fMRI) recordings (Freeman, Ahlfors and Menon, 2009).

1. B. Brain state space, state variables, state transitions

For functional connectivity we further conceive that at each of the postulated "very few short steps", the operation must result in neural activity having a spatiotemporal pattern. The pattern must be observed in fluctuations of potentials (electric, magnetic, hemodynamic) that are coherent over some contiguous collection, be they neurons, hypercolumns or modules. Each pattern must be stable long enough to be identified and measured, and it must recur sufficiently reliably in multiple trials of the action-perception cycle (Merleau-Ponty, 1942/1963, reduced by behaviorists to the stimulus-response reflex arc), in order to be collected in measurement space and categorized. At the microscopic level the patterns are observed in axon action potentials, that is, pulse trains of neurons in networks and measured as rates, intervals, and coincidences. At the mesoscopic level the patterns are observed in extracellular dendritic potentials of populations of neurons in areas of cortex and measured by digitizing the amplitudes. Depth electrodes serve to measure local field potentials (LFP); electrodes on cortical surfaces yield electrocorticograms (ECoG) (Fig. 01, A). At the macroscopic level the space-time patterns are observed with EEG and MEG scalp potentials, and diverse patterns of cerebral blood flow revealed by functional magnetic resonance imaging (fMRI) and related techniques. For evolving cortical populations the critical measures of functional connectivity are the magnitudes of correlation of activity between in well-defined frequency bands of the signals (Fig. 02, A) and the distances between cortical sites of recording, signifying the correlation lengths within spatially coherent patterns.

Fig. 02 near here

We make multichannel observations of spatial patterns simultaneously by using arrays of sensors and aggregate them in *n*-space, where *n* is the number of microscopic pulse trains, mesoscopic LFP/ECoG channels, macroscopic EEG/MEG channels, and fMRI voxels. Each train, channel and voxel contributes the coordinate axis of a dimension needed to create the *n*-space that defines an observable finite projection of the infinite brain state space. The range of observed values for all measures defines the magnitude of the *n*-space. Each measure that is simultaneously sampled at regular time intervals yields a state variable giving a point on its axis. The set of measurements at each time step determines an *n*-dimensional point in *n*-space. That point designates a spatial pattern to which all channels contribute, so the point and pattern represent the observed instantaneous state of the cortex.

A sequence of measurements gives a set of points forming a trajectory in state space that signifies a changing pattern. The Euclidean distance in *n*-space between successive samples in time gives the rate of change in the pattern. When the pattern is nearly fixed, the set of points forms a tight cluster. When the trajectory in *n*-space is projected into 2-space for graphic display, the trajectory appears as a line or curve with segments between and within clusters at the times of sampling. Each cluster represents the pattern of a transiently stable state. The trajectory between two clusters indicates a state transition. In dynamical terms each cluster manifests an attractor, and a set of clusters may represent a sequence of states that is variously described as an *attractor landscape* (Skarda and Freeman, 1987), a *metastable state* (Kelso, 1995; Bressler and Kelso, 2001; Kelso and Tognoli, 2006), a *chaotic itinerant trajectory* (Tsuda, 2001), the *connectome* forming the structural core of cerebral cortex (Sporns, Tononi and Kötter, 2005), the *Bayesian brain* minimizing free energy (Friston, 2009), the *testable taxonomy* of unconscious, preconscious and conscious states (Dehaene, Changeux et al., 2006), among others. The vector that defines each point is designated as an "order parameter" (Haken, 1983), because the pattern it represents describes the specific order of the instantaneous cortical state (Freeman and Vitiello, 2006, 2010).

The degree of order imposed is by the strength of interaction (synaptic feedback gain) among all of the neurons comprising a population. The order parameter is a vector that is evaluated by the pattern. The rate of change in the order parameter is given by the Euclidean distance in n-space between successive points, $D_e(t)$ (Fig. 02, B). It is an empirical scalar index of disorder (Freeman, 2004b); a low value signifies a cluster, and a high value signifies noise or a state transition through noise. The reciprocal, $1/ D_e(t)$, serves as an index of persisting order. A cluster with small increments reveals high probability of convergence of the trajectory to an attractor. A large step may reveal a state transition by a jump across the separatrix between two basins of attraction. Haken (1983) concluded that state transitions are essential to the mechanisms of information transfer between hierarchical levels. Each state transition by bifurcation provides one of the "very few short steps" by which brains mediate the action-perception cycle.

2. Relevant properties of connectivity in evolving scale-free networks

2. A. Types of probability distributions of connections

The distributions of numbers of connection as a function of the distances of transmission can be estimated by measuring the lengths of axons. The predicted distributions are best compared in log-log coordinates. In the original formulation of random graphs by Erdös and Renyí (1960) the probability of connections is uniform with distance (Fig. 03, A, lower line). In random cellular networks the connections are restricted to nearest or next-nearest neighbor nodes (e.g., Chua, 1998). In "small-world" graphs/networks a low percentage of the local connections is replaced with uniformly distributed long connections (Watts and Strogatz, 1998), which dramatically reduces the depth by bridging across many nodes. Small-world graphs/networks are related to cortical connectivity in the reported distributions of the lengths of axon projections (Fig. 03, B), which display predominantly local connections and increasingly sparse connections with increasing distance from the cell bodies (Fig. 03, A, dashed curve). The power-law distribution gives a straight line.

Fig. 03 near here

2. C. Power-law connectivity distributions and scale-free networks

Special significance is attached to the power-law distribution of connection distances, owing to the introduction of self-similarity at different scales of observation and measurement. The significance is found in the dynamical properties endowed by scale-free connectivity (Breakspear, 2004; Chen and Shi, 2004). The point raised here is that distributions of cortical connection lengths appearing to be exponential as commonly inferred (the convex dashed curve in Fig. 03, A) may actually be power-law (the slanted line) because of three experimental limitations on determinations of distributions of axonal lengths. First, for short distances the observations using light microscopy omit most unmyelinated axons, which in electron micrographs substantially outnumber the myelinated axons. Second, the observations of axon lengths in Golgi preparations are made in tissue sections of limited thickness (e.g., 300 microns, Fig. 03, B) in small mammals (here mouse). At the long end continuity is very difficult to follow in serial sections, leading to a deficit in the numbers of long connections. On the short end electron micrographs show that many unmyelinated terminal branches are smaller than the wavelengths used in optical microcopy, so they cannot be counted and can account for discrepancy in observed and power-law the distributions. Taking into account these experimental limitations, the data that have exponential distributions in semi-log coordinates may be consistent with power-law distributions in log-log coordinates. The theory offers a prediction for anatomists that the power-law model should be rigorously tested. A method to test functional transmission distance is considered in the next section.

3. Relevant properties of activity in evolving cortex

3. A. Origin, stabilization, and roles of background activity

Cortical neurons continually fire in “spontaneous” background activity, which is ubiquitous in all parts of functioning brains. Pulse trains yield autocorrelation functions and interval histograms that conform to a Poisson process with a dead time (Freeman, 1975/2004). The genesis of background activity has been modeled in detail for a population of interactive excitatory neurons in the olfactory bulb (a KIe set, Freeman and Erwin, 2008), in which the activity is sustained by the mutual synaptic excitation among excitatory neurons. The structural connectivity is sufficiently high that for each pulse emitted a neuron receives back on average more than one pulse, but owing to its refractory periods it might not respond. Hence the average magnitude of output is constrained for every neuron; it cannot remain silent, and it cannot fire above an average maximal rate. In physiological terms the background activity is everywhere locally stabilized homeostatically. The level of output is continuously adjusted by neuromodulation from brain stem histaminergic neurons that control the degree of arousal (Freeman, 2005).

In terms of nonlinear dynamics a non-zero point attractor everywhere locally controls the mean firing level of every neuron, which guarantees life-long viability through exercise. Upon linearization at the operating point, the transfer function of the local population is shown to have a pole on the negative real axis close to the origin of the complex plane. The stability is

demonstrated by electrical single shock stimulation of an afferent path. The impulse response is the probability of firing, which rises exponentially and decays at a rate proportional to response amplitude, which can be fitted with a sum of two exponential terms given by a 2nd order ordinary differential equation (ODE). The decay rate extrapolates to zero at zero input, proving that the population is governed by a stable point attractor that would give a pole at the origin in the absence of input. The increase in decay rate above zero at rest and in active behavioral states is due to the extrinsic background excitatory input on which the electrically excited test input is superimposed.

The conclusion is that the background activity is driven by mutual excitation (positive feedback among excitatory cells) that is self-stabilized by the refractory periods, so that the cortex is governed by a non-zero point attractor (Fig. 04). This attractor sustains a self-regulated state of criticality, in which the cortex is poised to jump from a receiving state to a transmitting state, but only when a conditioned stimulus is received (Fig. 1, A). The power spectral density, PSD, in the receiving state is linear in coordinates of log power vs. log frequency, $1/f^{\alpha}$, with a power-law exponent, $2 < \alpha < 4$. The form is determined by the background pulse input (white noise, $1/f^{0}$) after it has been filtered by the dendritic integration approximated by a 2nd order ODE. The output would be brown noise ($1/f^{2}$), but the refractory periods preventing firing remove power from the entire spectrum (Fig. 02, A) in proportion to the square of frequency (Freeman and Zhai, 2009). The result is “black noise” (Schroeder, 1991), which is characteristic of chaotic systems.

Fig. 04 near here

Populations of excitatory neurons are modeled by KIe sets, while populations of inhibitory neurons are modeled by KIi sets (Freeman, 1992). Both interactions are modeled by positive feedback loops, each subdivided into a receiving subset and a continually renewed transmitting subset and modeled with a 4th order ODE. The interaction of a KIe set with a KIi set gives negative feedback, which is modeled with an 8th order ODE (Chapter 5, Freeman, 1975/2004; Kozma and Freeman, 2001). The role of inhibition is to generate oscillations in dendritic synaptic potentials and their accompanying axonal pulse probability waves. The oscillations cover a spectrum (Fig. 02, A) from near zero to 3 Hz (delta), 3-7 Hz (theta), 7-12 Hz (alpha), beta (12-30 Hz), gamma (30-80 Hz), and epsilon (80-250 Hz). The latter is a new term to label the chatter of neural firing in the short loops of mutual excitation, by which positive feedback gives pulse intervals of 3-6 ms (Freeman, 1975/2004).). Cortical neurons require the excitatory bias to become re-excited on release from inhibition. In the rest state with minimal sensory input the EEG and ECOG oscillatory state variables have nearly Gaussian amplitude histograms, relatively flat autocorrelation functions, and broad spatial and temporal frequency distributions with power spectral densities (temporal, PSD_T, and spatial, PSD_X) conforming to power-law distributions in log-log coordinates (1/f).

The brain state at rest is symmetric, and the PSD reveals only the black noise. In the active state the symmetry is broken, bursts of oscillation emerge in the EEG and ECoG (Fig. 1, A), and peaks appear above the 1/f trend line in the PSD (Fig. 02, A). Linearization of the dynamics at the rest operating point yields transfer functions that again reveal the afore-mentioned pole at the origin of the complex plane. They also reveal an array of complex conjugate poles to the left of

the imaginary axis and of complex zeroes to the right of the axis having values that are constrained by the value of the pole at the origin (Chapter 5 in Freeman, 1975/2004). Calculation of the root loci of the poles in the complex plane predicts the existence of a limit cycle attractor for the KII set, which in a piecewise linear approximation in the small-signal range is represented by a pair of complex conjugate poles on the imaginary axis (Chapter 6 in Freeman, 1975/2004). This discovery leads to the hypothesis that the sudden emergence of a burst of activity in the gamma range occurs when control of the cortex temporarily transfers from the non-zero point attractor to the limit cycle attractor (Fig. 04) in a transition that resembles a subcritical Hopf bifurcation.

3. B. Cortical oscillations in response to input without and with state transitions

Input to cortex can change its activity in either of two ways. Perturbation by impulse input does not change the state of the cortex, because the cortex relaxes back to its prestimulus state while in doing so revealing its characteristic frequencies (Freeman, 1992). In this case the comparison of the perturbing input function with measures of the output functions define in terms of dynamics the operations by the cortex on the input to give the output. This approach is the basis for calculation of mutual information, cross-correlation, and transfer functions by piece-wise linearization (Freeman, 1975/2004). Particularly useful is the impulse input with electrical shocks, light flashes, auditory clicks, etc., giving “evoked potentials” that document the relaxation to the initial condition without change in state. Alternatively an input to cortex induces a state transition to an expanding oscillation (Shimoide and Freeman, 1995). The difference is crucial for understanding cortical dynamics. Both processes are initiated by input. Both can result in spatially coherent oscillation at a frequency in the beta-gamma range. Both oscillations are modulated spatially in both the amplitude and phase of the common carrier wave. In the relaxation process the amplitude and phase modulation (AM and PM) are imposed by the stimulus input in explicit symmetry breaking. In the state transition the AM and PM patterns emerge from the cortical connectivity that has been shaped by prior learning in spontaneous symmetry breaking (Freeman and Vitiello, 2006, 2010).

Demonstration of the relaxation process is by excitation of the olfactory bulb with single-shock afferent electrical stimulation of the olfactory nerve, which evokes a transient oscillation (an “evoked potential”) having the form of a damped cosine at the characteristic frequency of the bulbar negative feedback loop (Fig. 04, Mode 1e). When recorded from an array of electrodes on the surface, the ECoG oscillation at the common frequency has a spatial phase gradient across the bulb with slope and direction that correspond to the slow conduction velocity of the parallel unmyelinated axons forming the afferent nerve. The location of peak amplitude is determined by the stimulus site; when the stimulating electrode is moved to new locations in the parallel sheet of axons, the location of peak AM likewise shifts.

In contrast, inhalation triggers a volley of pulses from olfactory receptors in the nose that cause a sustained excitation of bulbar neurons. The result is the emergence of burst of activity called a wave packet having a characteristic carrier frequency that is shared throughout the bulb. The spatial pattern of amplitude modulation (the AM pattern) does not conform to the specific triggering input but is instead contingent upon learning. The spatial pattern in the phase of the carrier wave (the PM pattern) is not a plane wave sweeping across the bulb like the phase

gradient of the evoked potential. It is a radiating wave having a phase gradient with the shape of a cone. The direction and slope of the cone are determined not by the conduction velocities of the afferent axons but instead by the conduction velocities of intrabulbar axon collaterals (Freeman and Baird, 1987). These properties show that the wave packet in response to a conditioned stimulus is formed by a state transition. The burst of oscillation is not like the ringing of a bell when struck; it is like the ignition of an explosion (Fig. 04, Mode 2). In a distributed medium as in formation of a snowflake or raindrop that state transition does not take place everywhere simultaneously. It begins at a site of nucleation and spreads radially at an intrinsically determined velocity. Thus in the bulb the PM patterns are constrained by the conduction velocity of mitral collateral axons, and the reproducible AM pattern are determined by intrabulbar connectivity. A classifiable pattern emerges by spontaneous symmetry breaking only if the input contains a learned stimulus.

All of the primary sensory areas of neocortex share these properties. As in the bulb the AM patterned oscillations of neocortical wave packets in the beta-gamma range (20-80 Hz) result from a state transition only if the subject has been conditioned to respond to the stimuli, including the control background air with which it is familiarized. The oscillation evolves in a relatively narrow range, giving a peak in the PSD_T from a carrier wave with an AM pattern that is classifiable with respect to CS, and a PM pattern that manifests the location of the site of nucleation and the phase velocity. In neocortex the phase velocities (Freeman and Barrie, 2000) conform to the conduction velocities of corticocortical axons (Lohmann and Roerig, 1994; Swadlow, 1994). A sequence of amplitude patterns tends to repeat in the theta range (3-7 Hz) but with differing carrier frequencies in successive patterns. The near-invariance of frequency holds only within frames lasting ~0.1 s but with modulation of the frequency from each pattern to the next, so the PSD_T computed over epochs ≥1 s has a relatively broad peak (Fig. 02, A) spanning the high beta and low gamma ranges.

Most significantly, the AM pattern lacks invariance with respect to its fixed CS. When the CS is held constant but its meaning is changed, the AM pattern changes irreversibly (Freeman and Grajski, 1987). The same result holds for all sensory areas of neocortex as well (Barrie, Freeman and Lenhart, 1996). We conclude that the first of von Neumann's "very few short steps" in the sensory systems is the transduction of sensory energy in various forms into information-bearing action potentials, and that the second step is the state transition on destabilization of the sensory cortices, which leads to the construction of an activity pattern that retrieves the knowledge about a CS that is stored in synaptic weights. The several sensory cortices send their AM patterns into the limbic system, where in von Neumann's third step they are integrated into a multisensory percept (gestalt). This review is restricted to his second step.

3. C. Bifurcations, state transitions and chaos

The olfactory system has multiple components. The three largest parts suffice to model the system dynamics: the olfactory bulb (OB), prepyriform cortex (PC) and anterior nucleus (AON) (Freeman, 1992). When surgically isolated from each other and stimulated by impulse input, the OB, PC and AON reveal point attractors by giving damped cosines at step onset, each with its characteristic frequency. The three frequencies are incommensurate (Kozma and Freeman, 2001), so the parts cannot by synchronized at any one frequency. The parts are coupled by

feedback pathways with delays, some of which are excitatory and tend continually to increase the system activity by positive feedback, while others are inhibitory and tend to sustain system oscillations by negative feedback. All interactions are limited by the thresholds and refractory periods of the neurons. A dynamical model of the system consists of three interconnected KII sets, KIIob, KIIpc, and KIIaon, with a bias-generating KIe set at the input, forming a KIII set. The solutions to the matrix of ODE suffice to simulate the background activity, the impulse responses of the component populations, the induced bursts of transient limit cycle oscillation (Fig. 01, A) (Kay et al., 1995), and genesis of simple and complex partial epileptic seizure spikes (Fig. 01, B) (Freeman, 1986), from which we infer that the noise-free model has multiple Lyapunov exponents, most of which are negative or zero, and at least one of which is positive.

The most glaring deficiency is the failure to model the 1/f power-law form of the PSD. The reason is clear, that the continuum of the real 1/f form implies an infinite dimensional system, whereas the K-sets are rational approximations for implementation of low-dimensional systems on digital platforms. The parameters of the approximations can be tuned to approach the 1/f form (Chang, Freeman and Burke, 1998), but in doing so the model becomes progressively more brittle, essentially by the addition of more basins of attraction. In effect the attractor landscape begins to resemble rabbit fur, owing to the proliferation of attractors, resulting in attractor crowding. The basins of attraction approach the size of the digitizing step, so that well within a fraction of a second the system placed in the basin of a chaotic attractor steps our into a neighboring basin of a point or limit cycle attractor. Empirically the remedy is provided by additive noise (Chang and Freeman, 1998) in two forms. One form is low-level random numbers applied to each input channel in the KIe array uncorrelated between channels; the other is a single channel of low level random numbers given to the KIIaon. In effect the KIII landscape is smoothed from rabbit fur to alligator skin, enabling a manageable number of limit cycle attractors to coexist (Fig. 01, B). The additive noise solves the problem of the infinite sensitivity of chaotic systems to changes in the initial conditions and ensures metastability in both brains and brain models (Kozma and Freeman, 2003). In effect the ODE as implemented on digital platforms become stochastic difference equations. Multiplicative noise also plays a role in the homeostatic regulation of input gain to compensate for wide fluctuations in the intensity of sensory input. This janitorial operator is essential for signal normalization and range compression. It has been documented in studies that deserve more recognition than it has received (Freeman, 1974; Chang and Freeman, 1999).

Clearly brains are not deterministic, and attempts to evaluate correlation dimensions and Lyapunov exponents using EEG and ECoG are certain to be confounded by noise (Rapp, 1993). The modulation of deterministic chaos by additive noise (Freeman et al., 1997) creates a tool, stochastic chaos (Freeman, 2000). The formalism encourages the search for nonconvergent solutions for matrices of ODE to complement point and limit cycle attractors, taking advantage of the theories of metastability (Kelso, 1995; Kelso and Tognoli, 2006), large-scale networks (Bressler and Menon, 2010), and chaotic itinerancy (Tsuda, 2001). The principal barrier to exploitation is the excessive run time required for numerical solutions of ODE, which might some day be circumvented by implementation of K-sets in analog VLSI (Principe et al., 2001) and in random graph theory using neuropercolation theory (Kozma et al., 2005; Freeman et al., 2009).

4. Conclusions: Guidance by chaos theory of further biological experimentation

4. A. Applications of noise-modulated deterministic chaos

Even though brain dynamics does not conform to low-dimensional chaos, the theory provides the guidance needed to construct and evaluate matrices of ODE with which to simulate brain functions in the cognitive realms of perception and choice. The non-convergent solutions of the ODE do suffice to simulate a wide range of spontaneous, evoked, and induced wave forms including the genesis of simple and complex partial epileptic seizures (Fig. 01, B). More importantly when the KIII set is expanded into multiple 2-D layers of the several interactive KIe and KIi layers, the model performs pattern classification with exceptionally high levels of success, beginning with olfactory stimuli such as kinds of tea, Yang et al., 2006), and extending to quality control of machine screws in industry (Yao et al., 1991), Japanese vowel sounds (Shimoide and Freeman, 1995), EEG patterns (Kozma and Freeman, 2002), face recognition (Li et al., 2004), all 36 alphanumeric characters with an 8x8 array (Li et al., 2006), and EEG patterns in seizure (Ruiz et al., 2009) and hypoxia (Hu et al., 2006), outperforming conventional neural networks in requiring small training sets (typically 5 to 10 examples), one-step convergence by phase transition rather than asymptotic approach by gradient descent, and memory capacity increasing geometrically with the number of nodes (Kozma and Freeman, 2001; Kozma et al., 2005; Ilin, Kozma and Werbos, 2008). Further uses of multisensory pattern classification are achieved by conjoining three KIII sets to form a KIV set, which simulates the dynamics of goal-directed behavior of primitive vertebrates by constructing multisensory percepts (gestalts) for making decisions (Kozma, Freeman and Erdí, 2003) and guiding navigation (Kozma and Freeman, 2003). The full-scale implementation in a prototype of a Martian rover SSR2K (Kozma, 2008) pioneered the field of intentional robotics.

4. B. Neuroanatomy and neuroembryology

In terms of hierarchical dynamics the allocortex is better described not as three-layered but as a single functional layer, and neocortex not as six-layered but as having two functional layers. The localized groups in Layers III to IV constitute modules for specialized information processing. The embedding neuropil in Layers I, II, V and VI (Fig. 06) forms a continuum over each cerebral hemisphere. Unlike allocortical neuropil, which has discontinuities in connection densities that segregate major areas from each other and from neocortex, the embedding neuropil of neocortex in each hemisphere forms a unified organ that enables the radial spread of activity by synaptic and diffusion-mediated communication. Evidence for this continuity is provided the spreading depression of Leão (Bures, Buresova and Krivánek, 1974) from any site in the neocortex in each hemisphere but not to the other hemisphere or outside the neocortex. However, the mechanism of spreading depression is non-synaptic, nearest-neighbor. New data are needed to verify the hypothesis that connection distances have power-law distributions (Fig. 02), and to map the axonal distributions to provide the kernels needed to model the spatial integral transforms performed by divergent and convergent pathways. At present the best-documented example of a non-topographic, divergent-convergent projection is the lateral olfactory tract from the olfactory bulb to the prepyriform cortex (Freeman, 1975/2004).

Most analyses of anatomical data have emphasized point-to-point networks, as in the classic

meta-study by Fellemin and Van Essen (1991) of connectional architecture in visual cortex. These linkages are very important for the organization of the vectorial order parameters of mesoscopic and macroscopic AM patterns; however, they do not address the connectivity required for the long-range coherence and rapid state transitions revealed by carrier waves. Braitenberg and Schüz (1998) wrote: "A recent hypothesis by Miller (1996), based on differences in both connectivity patterns and spontaneous activity between upper and lower layers, assigns to the upper layers the role of a neuronal 'library', storing most of the information encoded by assemblies … while the lower layers are assumed to *catalyze* the process of assembly formation" (p. 150). Long cortico-cortical connections are not randomly distributed within the territory that they innervate. Instead they are distributed in patches with high local connection density, with intervening regions having few connections (Malach, 1994). Kaas (1987) wrote: "Generalizing from cats and monkeys it appears that the evolutionary advance in brain organization is marked by increases in the numbers of unimodal sensory fields, not by increases in multimodal association cortex as traditionally thought" (p. 147). Therefore Layers III-IV provide highly textured modules, while the embedding neuropil in Layers I, II, V and VI provides not only the connectivity needed for rapid integration of macroscopic modular activity in the encompassed clusters but also the uniformity and unity of neocortical anatomy that has often been noted by neuroanatomists. What is needed is the measurement and statistical analysis of the holistic organization of long connections in the manner pursued by Bok (1959), and explication of the neuroembryological rules that govern formation of integrative systems, the developmental processes by which scale-free connectivity emerges in neocortex. Gulyas (2006) has demonstrated the ability to generate scale-free networks using local information in bottom-up construction. Close collaboration between network theorists and neuroembryologists will be needed to advance in this direction.

4. C. Brain imaging combining structural and functional MRI, EEG and MEG

The inference that foci seen with fMRI are signs of coordinated modules may best be tested by combining hemodynamic imaging with EEG and MEG (Logothetis, 2008; Freeman, Ahlfors and Menon, 2009; Bressler and Menon, 2010). Preliminary data indicate that the necessary brain-wide macroscopic wave packets with beta carrier frequencies are found in human volunteers engaged in cognitive tasks (Ruiz et al., 2010). Quantitative assays with a 64x1 linear array at 3 mm spacing on the scalp have shown (Freeman, Burke and Holmes, 2003) that re-synchronization of both beta and gamma activity recurs at rates in the theta and alpha ranges, commonly over correlation distances on the scalp of several cm and occasionally over the full length of the array, 19 cm. EEG data from intracranial arrays support the inference that cortical dynamics is scale-free, so that brains ranging 10^4 in mass from mice to whales have the capacity for widespread state transitions that rapidly and repeatedly re-synchronize beta and gamma oscillations carrying AM patterns correlated with cognitive processes. Wang and Chen (2002) in studies of the temporal dynamics have shown that above a certain threshold of connection density, a scale-free network can undergo an abrupt state transition and resynchronize globally no matter how large its diameter. Use of the Hilbert transform to calculate measures of beta-gamma analytic power is optimal, because the state variable thereby derived as an index for power is more closely related to the demands for metabolic energy than are the amplitudes of low frequencies (alpha, theta, delta) (Logothetis, 2008).

5. References

*Published in the International Journal of Bifurcation and Chaos
*Freeman, WJ (1992) Tutorial in Neurobiology: From Single Neurons to Brain Chaos. Int J Bifurc Chaos 2: 451-482.
*Kay LM, Shimoide K, Freeman WJ (1995) Comparison of EEG time series from rat olfactory system with model composed of nonlinear coupled oscillators. Int J Bifurc Chaos 5: 849-858.
*Chang H-J, Freeman WJ (1998) Biologically modeled noise stabilizing neurodynamics for pattern recognition. Int J Bifurc Chaos 8 (2), 321-345.
*Chang H-J, Freeman WJ (1999) Local homeostasis stabilizes a model of the olfactory system globally in respect to perturbations by input during pattern classification. Int J Bifurc Chaos 8: 2107-2123.
*Freeman WJ (1999) Noise-induced first-order phase transitions in chaotic brain activity. Int J Bifurc Chaos 9: 2215-2218.
*Freeman WJ (2000) Characteristics of the synchronization of brain activity imposed by finite conduction velocities of axons. Special Issue on Synchronization, Kurtz J (ed.) Int J Bifurc Chaos 10: 2307-2322.
*Kozma R, Freeman WJ (2001) Chaotic resonance: Methods and applications for robust classification of noisy and variable patterns. Int J Bifurc Chaos 10: 2307-2322. (Cover Figure)
*Freeman, W.J. (2003a) A neurobiological theory of meaning in perception. Part 1. Information and meaning in nonconvergent and nonlocal brain dynamics. Int J Bifurc Chaos 13: 2493-2511. http://repositories.cdlib.org/postprints/3348
http://repositories.cdlib.org/postprints/2355
*Freeman, W.J. (2003b) A neurobiological theory of meaning in perception. Part 2. Spatial patterns of phase in gamma EEG from primary sensory cortices reveal the properties of mesoscopic wave packets. Int J Bifurc Chaos 13: 2513-2535.
http://repositories.cdlib.org/postprints/3343
*Freeman WJ, Gaál G, Jornten R (2003) A neurobiological theory of meaning in perception. Part 3. Multiple cortical areas synchronize without loss of local autonomy. Int J Bifurc Chaos 13: 2845-2856. http://repositories.cdlib.org/postprints/3344
*Freeman WJ, Burke BC (2003) A neurobiological theory of meaning in perception. Part 4. Multicortical patterns of amplitude modulation in gamma EEG. Int J Bifurc Chaos 13: 2857-2866. http://repositories.cdlib.org/postprints/3345
*Freeman WJ, Rogers LJ (2003) A neurobiological theory of meaning in perception. Part 5. Multicortical patterns of phase modulation in gamma EEG. Int J Bifurc Chaos 13: 2867-2887. http://repositories.cdlib.org/postprints/3346
*Freeman W.J. (2004) How and why brains create meaning from sensory information. Int J Bifurc Chaos 14: 513-530.
http://repositories.cdlib.org/postprints/1689
*Li X, Li G, Wang L, Freeman WJ (2006) A study on a bionic pattern classifier based on olfactory neural system. Int J Bifurc Chaos 16(8): 2425-2434.

Barrie JM, Freeman WJ, Lenhart M (1996) Modulation by discriminative training of spatial patterns of gamma EEG amplitude and phase in neocortex of rabbits. J Neurophysiol 76:

520-539.
Bok ST (1959) Histonomy of the Cerebral Cortex. Amsterdam: Elsevier.
Braitenberg V, Schüz A (1998) Cortex: Statistics and Geometry of Neuronal Connectivity, 2nd ed. Berlin: Springer-Verlag.
Breakspear M (2004) Dynamic connectivity in Neural systems: Theoretical and empirical considerations. Neuroinformatics 2(2): 205-225.
Bressler SL, Kelso JAS (2001) Cortical coordination dynamics and cognition. Trends Cogn Sci 5: 2-36.
Bressler SL, Menon V (2010) Large-scale networks in cognition: emerging methods and principles. Trends Cogn Sci 14: 277-290.
Bures J, Buresová O, Krivánek J (1974) The Mechanism and Applications of Leão's Spreading Depression of Electroencephalographic Activity. New York: Academic Press.
Chang H-J, Freeman WJ, Burke BC **(**1998) Optimization of olfactory model in software to give 1/f power spectra reveals numerical instabilities in solutions governed by aperiodic (chaotic) attractors. Neural Networks (11: 449-466.
Chen Q, Shi D (2004) The modeling of scale-free networks. Physica A 333: 240-248.
Chua LO (1998) CNN. A Paradigm for Complexity. Singapore: World Scientific.
Dehaene S, Changeux JP, Naccache L, Sackur J, Sergent C (2006) Conscious, preconscious, and subliminal processing: a testable taxonomy. Trends Cogn Sci 10: 204–211.
Erdös P, Renyí A (1960) On the evolution of random graphs. Publ. Math. Inst. Hung. Acad. Sci. 5: 17-61.
Fellemin DJ, Van Essen DC (1991) Distributed hierarchical processing in the primate cerebral cortex. Cerebral Cortex 1: 1-47.
Freeman WJ (1960) Correlation of electrical activity of prepyriform cortex and behavior in cat. J Neurophysiol 23: 111-131.
Freeman WJ (1974) Attenuation of transmission through glomeruli of olfactory bulb on paired shock stimulation. Brain Research 65: 77-90.
Freeman WJ (1975) Mass Action in the Nervous System. New York: Academic Press. Electronic version 2004: http://sulcus.berkeley.edu/MANSWWW/MANSWWW.html
Freeman WJ (1986) Petit mal seizure spikes in olfactory bulb and cortex caused by runaway inhibition after exhaustion of excitation. Brain Research Reviews 11:259-284.
Freeman WJ (1987) Simulation of chaotic EEG patterns with a dynamic model *of* the olfactory system. Biol Cybern 56: 139–50. Fig 12
Freeman WJ (2000) A proposed name for aperiodic brain activity: Stochastic chaos. Neural Networks 13: 11-13
Freeman WJ (2004a) Origin, structure, and role of background EEG activity. Part 1. Analytic amplitude. Clin Neurophysiol 115: 2077-2088. http://repositories.cdlib.org/postprints/1006
Freeman WJ(2004b) Origin, structure, and role of background EEG activity. Part 2. Analytic phase. Clin Neurophysiol 115: 2089-2107. http://repositories.cdlib.org/postprints/1486.
Freeman WJ (2005) NDN, volume transmission, and self-organization in brain dynamics. J Integrative Neuroscience 4 (4): 407-421
Freeman WJ (2006) Definitions of state variables and state space for brain-computer interface. Part 1. Multiple hierarchical levels of brain function. Cogn Neurodyn 1(1): 3-14. http://dx.doi.org/10.1007/s11571-006-9001-x
http://repositories.cdlib.org/postprints/33712007
Freeman WJ (2007) Definitions of state variables and state space for brain-computer interface.

Part 2. Extraction and classification of feature vectors. Cogn Neurodyn 1(2): 85-96. http://www.springerlink.com/content/w7737h5tg6551888/ http://repositories.cdlib.org/postprints/3372

Freeman WJ, Ahlfors SM, Menon V (2009) Combining EEG, MEG and fMRI signals to characterize mesoscopic patterns of brain activity related to cognition. Int J Psychophysiol 73(1): 43-52. http://repositories.cdlib.org/postprints/3386

Freeman WJ, Baird B (1987) Relation of olfactory EEG to behavior: Spatial analysis: Behav Neurosci 101: 393-408.

Freeman WJ, Barrie JM (2000) Analysis of spatial patterns of phase in neocortical gamma EEGs in rabbit. J Neurophysiol 84: 1266-1278.

Freeman WJ, Burke BC, Holmes MD (2003) Aperiodic phase re-setting in scalp EEG of beta-gamma oscillations by state transitions at alpha-theta rates. Human Brain Mapping 19(4): 248-272. http://repositories.cdlib.org/postprints/3347

Freeman WJ, Chang H-J, Burke BC, Rose PA, Badler J (1997) Taming chaos: Stabilization of aperiodic attractors by noise. IEEE Trans Circuits Systems 44:989-996.

Freeman WJ, Erwin H (2008) Freeman K-set. Scholarpedia, 3(2): 3238 http://www.scholarpedia.org/article/Freeman_K-set

Freeman WJ, Grajski, K.A. (1987) Relation of olfactory EEG to behavior: Factor analysis: Behav Neurosci 101: 766-777.

Freeman WJ, Kozma R, Bollobás B, Riordan O (2009) Chapter 7. Scale-free cortical planar network, in: Handbook of Large-Scale Random Networks. Series: Bolyai Mathematical Studies, Bollobás B, Kozma R, Miklös D (Eds.), New York: Springer, Vol. 18, pp. 277-324. http://www.springer.com/math/numbers/book/978-3-540-69394-9

Freeman WJ, Vitiello G (2006) Nonlinear brain dynamics as macroscopic manifestation of underlying many-body field dynamics. Physics of Life Reviews 3: 93-118. http://dx.doi.org/10.1016/j.plrev.2006.02.001, http://repositories.cdlib.org/postprints/1515

Freeman WJ, Vitiello G (2010) Vortices in brain waves. International Journal Modern Physics B, Vol: 24 (17): pp. 3269-3295. http://dx.doi.org/10.1142/S0217979210056025

Freeman WJ, Zhai J (2009) Simulated power spectral density (PSD) of background electrocorticogram (ECoG). Cognitive Neurodynamics 3(1): 97-103. http://dx.doi.org/10.1007/s11571-008-9064-y

Friston K (2009) The free-energy principle: a rough guide to the brain? Trends Cogn Sci 13(7): 293-301. doi:10.1016/j.tics.2009.04.005

Haken H (1983) Synergetics: An Introduction. Berlin: Springer-Verlag

Hu M, Li J, Li G, Tang X, Freeman WJ (2006) Normal and hypoxia EEG recognition based on a chaotic olfactory model. LNCS Vol 3973: 554-559, doi: 10.1007/11760191

Ilin R, Kozma R, Werbos PJ (2008) Beyond backpropagation and feedforward models: a practical training tool for a more efficient universal approximator. IEEE Trans Neur Netw 19(3), 929-937.

Kaas JH (1987) The organization of neocortex in mammals: implications for theories of brain function. Ann Rev Psychol 38: 129-152.

Kelso JAS (1995) Dynamic Patterns: The Self Organization of Brain and Behavior. Cambridge MA: MIT Press.

Kelso JAS, Tognoli E (2006) Metastability in the brain. Neural Networks IJCNN'06: 363-368. doi: 10.1109/IJCNN.2006.246704

Kozma R (2003) On the constructive role of noise in stabilizing itinerant trajectories on chaotic dynamical systems. Chaos 11(3): 1078-1090.
Kozma R, Freeman WJ (2002) Classification of EEG patterns using nonlinear dynamics and identifying chaotic phase transitions. Neurocomputing 44: 1107-1112.
Kozma R, Freeman WJ (2003) Basic principles of the KIV model and its application to the navigation problem. J Integr Neurosci 2(1): 125-146.
Kozma R, Freeman WJ, Erdí P (2003) The KIV model – nonlinear spatiotemporal dynamics of the primordial vertebrate forebrain. Neurocomputing 52-54: 819-826.
Kozma R, Huntsberger T, Aghazarian H, Tunstel E, Ilin R, Freeman WJ (2008) Implementing intentional robotics principles using SSR2K platform. Advanced Robotics 22(12): 1309-1327.
Kozma R, Puljic M, Bollobas, B, Balister, P, Freeman, WJ (2005) Phase transitions in the neuropercolation model of neural populations with mMixed local and non-local interactions. Biol. Cybernetics, 92(6), 367-379.
Li G, Li L, Wang W, Freeman WJ (2004) Face recognition using a neural network simulating olfactory systems. LNCS Vol 3972: 93-97.
Logothetis NK (2008) What we can do and what we cannot do with fMRI. *Nature* 453: 869-878. doi:10.1038/nature06976
Lohmann H, Roerig B (1994) Long-range horizontal connections between supragranular pyramidal cells in the extrastriate visual cortex of the rat. J Comp Neurol 344: 543-558.
Malach R (1994) Cortical columns as devices for maximizing neuronal diversity. TINS 17: 101-104.
Merleau-Ponty M (1942/1963) The Structure of Behavior. Fischer AL (trans) Boston: Beacon.
Miller R (1996) Neural assemblies and laminar interactions in the cerebral cortex. Biol Cybern 75: 253-261.
Principe, J.C., Tavares, V.G., Harris, J.G. and Freeman, W.J. (2001) Design and implementation of a biologically realistic olfactory cortex in analog VLSI. Proceedings IEEE 89: 1030-1051.
Rapp P (1993) Chaos in the neurosciences: Cautionary tales from the frontier. Biologist 40: 89-94.
Ruiz Y, Li G, Freeman WF, Gonzalez E. (2009) Detecting stable phase structures on EEG signals to classify brain activity amplitude patterns. J Zhejiang Univ 10(10):1483-1491
Schroeder M (1991) Fractals, chaos, power laws. Minutes from an infinite paradise. WH Freeman, San Francisco
Shannon CE (1948) A mathematical theory of communication. Bell System Tech. J. **27**: 379-623.
Shimoide K, Freeman WJ (1995) Dynamic neural network derived from the olfactory system with examples of applications. IEICE Transaction Fundamentals E-78A: 869-884.
Skarda, C.A., Freeman WJ (1987) How brains make chaos in order to make sense of the world. Behavioral and Brain Sciences 10: 161-195.
Sporns O, Tononi G, Kötter R (2005) The human connectome: A structural description of the human brain. PLoS Comput Biol 1: 245–251. doi:10.1371/ journal.pcbi.0010042
Swadlow HA (1994) Efferent neurons and suspected interneurons in motor cortex of the awake rabbit: axonal properties, sensory receptive fields and subthreshold synaptic inputs. J Neurophysiol 71: 437-453.
Tsuda I (2001) Towards an interpretation of dynamic neural activity in terms of chaotic dynamical systems. Behav Brain Sci 24:793-810.

von Neumann J (1958) The Computer and the Brain. New Haven CT: Yale UP.
Wang XF, Chen GR (2003) Complex networks: small-world, scale-free and beyond. IEEE Trans Circuits Syst, 31: 6-20.
Watts DJ, Strogatz SH (1998) Collective dynamics of 'small-world' networks. Nature 393: 440-442, 1998
Yang X, Fu J, Lou Z, Wang L, Li G, Freeman, WJ (2006) Tea classification based on artificial olfaction using bionic olfactory neural network. In: Wang X, Zhang L, Sun Y, Kim K-B, Lu W, Wu Y, Li B, Wang J, Wang W, Wang, H (Eds.): Advances in Neural Networks – ISNN 2006. Lecture Notes in Computer Science. Heidelberg: Springer, pp. 343–348.
Yao Y, Freeman WJ, Burke B, Yang Q (1991) Pattern recognition by a distributed neural network: An industrial application. Neural Networks 4: 103-121.

Figures and Legends

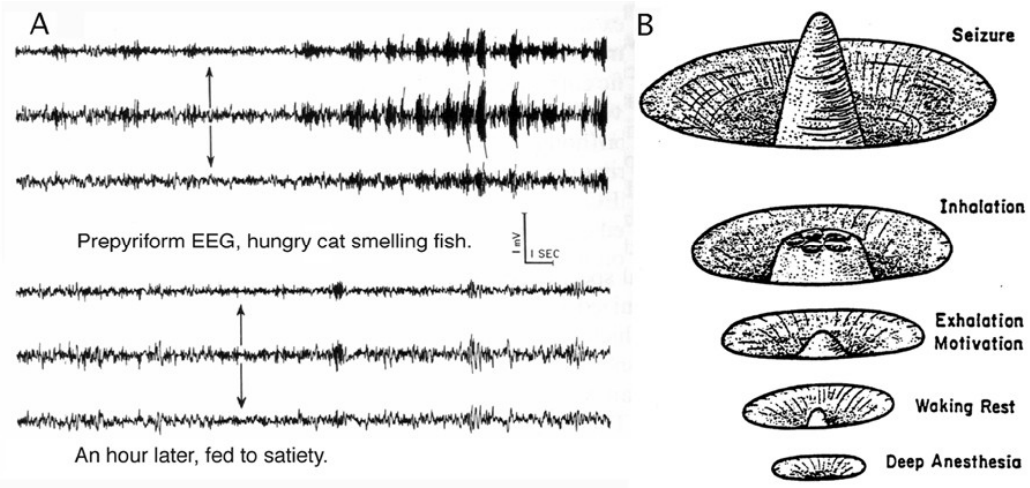

Fig. 01. A. The bipolar ECoG recording came from an electrode pair straddling the prepyriform cortical dipole field, first when the subject was habituated to a closed box. The upper signals were from the cat when given a whiff of fish when it was hungry, and the lower signals were when it had been fed to satiety. From Fig. 2, p. 115 in Freeman (1960) **B.** A phase portrait of the olfactory system was constructed from recordings of the ECoG in the range of designated states. In the aroused state ('motivation') control of the ECoG repeatedly shifted between a non-zero point attractor during exhalation and a landscape of limit cycle attractors emergent during inhalation, each having its basin of attraction in the landscape. When the phase transition took place, the control of cortex was shifted from a point attractor to one of the limit cycle attractors representing one of the Bayesian priors that sensitized the bulb to a particular expected odorant stimulus. From Fig. 12, p. 145 in Freeman (1987)

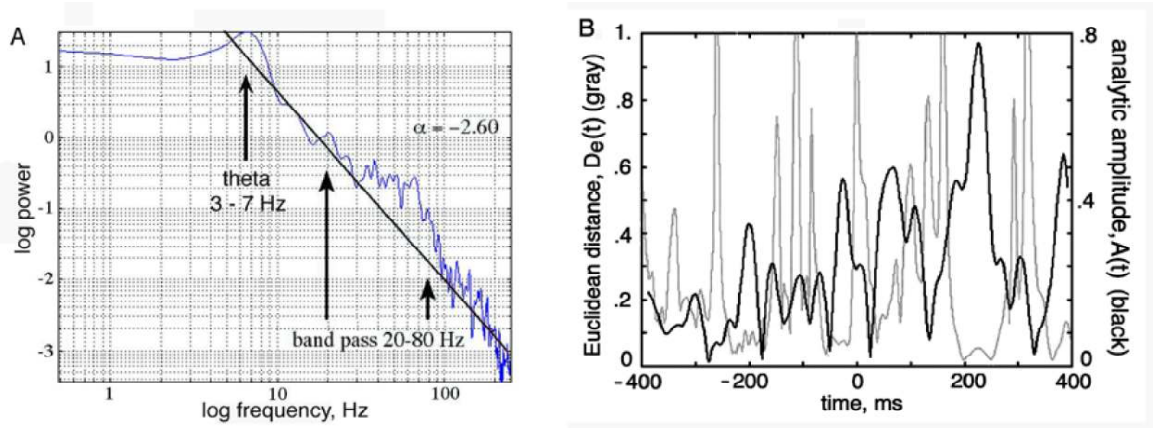

Fig. 02. A. The temporal power spectral density (PSD_T) had 1/f form in rest state but excess power above the trend line in theta and beta-gamma ranges during active states, implying increased order. (Freeman, 2004a, Fig. A1.02, A) **B.** A(t) (black) and $1/D_e(t)$ (gray) from the Hilbert transform on trials with CS (onset at 0 ms) showed intermittent frames with decreased rate of pattern change (gray curve), increased amplitude (black curve), and near-invariant instantaneous frequency (constant rate of increase in analytic phase), which imply increased order during frames between state transitions (Freeman, 2004b, Fig. 1.02). $D_e(t)$ in B shows that ECoG power in each burst is concentrated in a narrow frequency band, so that frequency modulation across several bursts explains the broad peak in A.

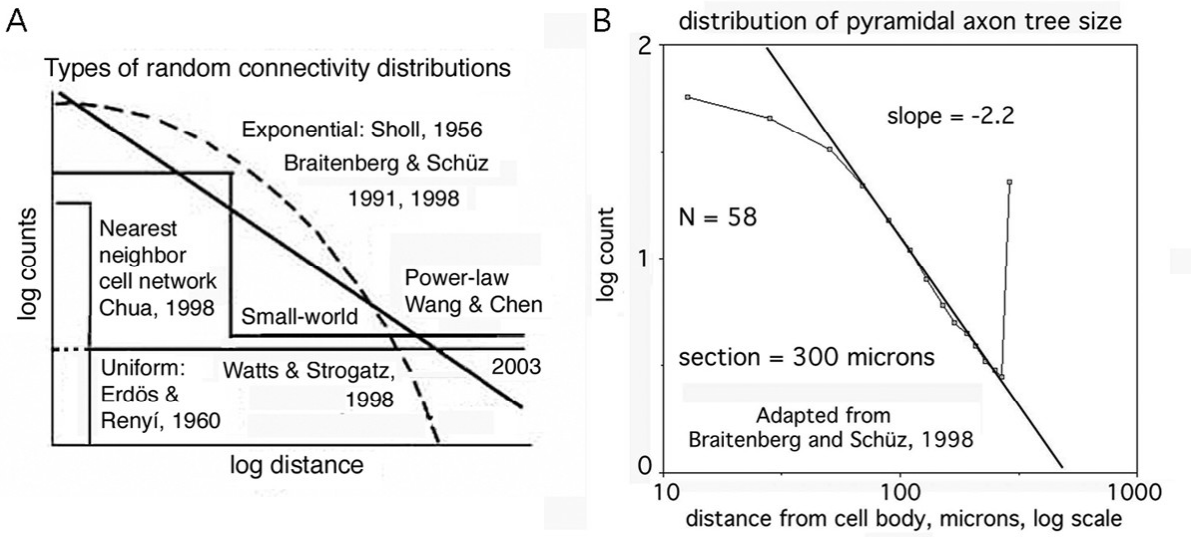

Fig. 03, A. Distributions of the numbers of connections as a function of distances are schematized in log-log coordinates. The straight line indicates 1/f. **B.** An example is shown of the distribution of measurements of lengths of axons that were made in histological sections of Golgi preparations of mouse cortex. The vertical line shows the count of axons that left the tissue section and couldn't be followed to the axon ends. The data were re-plotted in log-log coordinates. Adapted from Braitenberg and Schüz (1998)

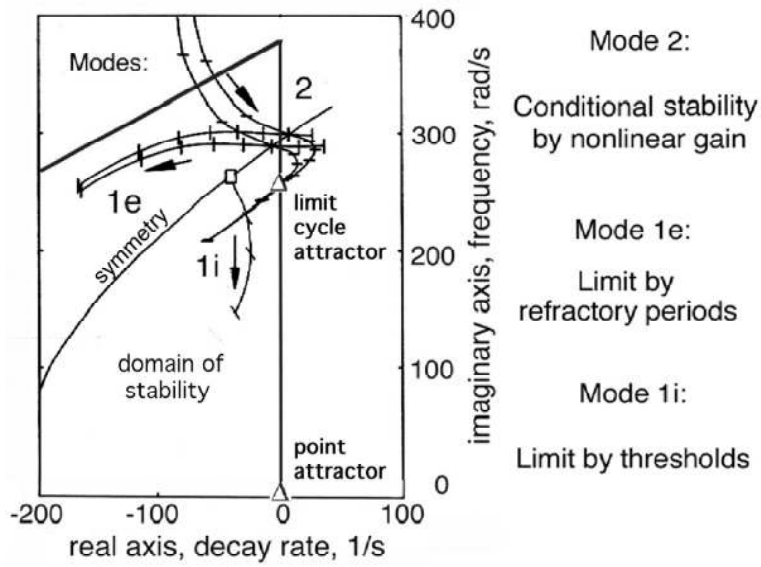

Fig. 04. The diagram displays root loci of the critical complex conjugate pole in the upper half of the complex plane closest to the imaginary axis and therefore dominating the impulse response. The root loci are plotted by repeated solutions of linearized ODEs fitted to impulse responses of the cortex. The arrows show the direction of displacement with increasing amplitude of activity. Mode 1e shows impulse responses with excitatory bias, and Mode 1i with inhibitory bias, both in explicit symmetry breaking. Mode 2 shows the tendency to spontaneous symmetry breaking on approach to the limit cycle attractor on the imaginary axis with increasing amplitude, which for the linear approximation represents a singularity. The state transition begins when the sign of the real part of the complex pole changes from – to +. From Fig. 6.30 on p. 388, with equations for the root loci in Chapter 6, Freeman (1975/2004)